Received: 28 February 2022 | Revised: 03 April 2022 | Accepted: 03 April 2022
DOI: 10.22034/ecc.2022.335455.1396
Eurasian Chemical Communications
SAMI

FULL PAPER

Novel naphthalene-derived coumarin composites: synthesis, antibacterial, and antifungal activity assessments

Sarah Ahmed Waheed* | **Yasser Fakri Mustafa**

Pharmaceutical Chemistry Department, College of Pharmacy, University of Mosul, Mosul, Iraq

Composites with a coumarin-based chemical structure have sparked a lot of interest in the scientific community. This is because of their diverse structural properties and also, their wide range of biological activities. In this work, eight novel naphthalene-derived coumarin composites were synthesised, confirmed by various spectrophotometers, and assessed for anti-bacterial and anti-fungal activities. The pharmacokinetic parameters were evaluated *in silico* using pre-ADMET, a free online program. The antimicrobial activity was tested using the method of broth-dilution towards six aerobic gram-negative bacterial strains (*Klebsiella pneumonia, Pseudomonas aeruginosa, Escherichia coli, Haemophilus influenzae, Shigella dysenteriae, and Salmonella typhi*), four anaerobic bacterial strains (*Prevotella melaninogenica, Bacteroides fragilis, Clostridium perfringens, and Fusobacterium necrophorum*), as well as two fungal strains (*Aspergillus niger* and *Candida albicans*). The safety profile was inspected by testing the toxicity for normal flora bacteria. Pharmacokinetic investigations demonstrated that the synthesised naphthalene-derived coumarin composites have good penetration across the GIT mucosa and most of them have poor penetration across the blood-brain barrier. These findings suggest good oral bioavailability along with low neurological toxicity profiles. The evaluations of the antimicrobial activity revealed that our composites have a weak bactericidal influence on gram-negative aerobic as well as anaerobic bacteria. The foremost discovery in this report was that most of these composites have an extremely potent fungicidal influence. The authors hope that this realization, along with the apparent safety of these compounds, can be utilized in the coming time for the production of new powerful fungicidal influence drugs.

***Corresponding Author:**
Sarah Ahmed Waheed
Email: sarah.ahmed@uomosul.edu.iq
Tel.: 07701690707

KEYWORDS

Synthesis; antimicrobial; broth-dilution; bactericidal influence; fungicidal influence.

Introduction

Resistant pathogens have developed novel fighting processes continue to pose a danger to our capacity to cure infective illnesses. The increasing worldwide expansion of multi-or even pan-resistant microbes, or “superbugs” produces diseases that are refractory to current antimicrobial medications. This leads to more cases of severe microbial infections that have been threatening humanity. This resistance arises from the non-judgemental use of antimicrobial agents over many years. Scientists, pharmaceutical chemists, and other medical researchers are working side by side for the great purpose of preparing new consolidations. The newly developed agents can restore control to our hands by

designing novel agents should have a high ability to demolish these resistant tiny creatures along with as little resistance potential as possible. The efforts have been made to identify such agents in nature and convert them into appropriate medicines to treat these resistant infections [1,2].

Coumarins constitute an interesting group of compounds. Researchers have been focused for decades on studying their crucial biological features and preparing analogues for therapeutic applications. Coumarins are a class of heterocyclic compounds with a benzopyrone core structure. These molecules offer a number of appealing properties make them an important part of drug research and innovation. In addition to their multifarious bioactivities, they have a simple structure, low molecular weight, good bioavailability, excellent safety profile, and high solubility in many solvent systems. Their skeletons have been employed as a precursor in the preparation of biologically active heterocyclic compounds with anti-inflammatory, anti-microbial, anti-tumour, painkiller, antioxidant, hypoglycemic, anticoagulant, and many other activities [3–11].

Naphthalene-derived coumarin composites are considered promising scaffolds in the future for the production of modern drugs with favourable biological activities. These composites are coumarins with phenyl groups bonding to either 3,4-,5,6-, 6,7-, or 7,8-positions, resulting in a slew of appealing bioactivities [12]. They are a prospective family of new compounds due to the make-up of their structure with an expanded π-electron arrangement. Three subfamilies of naphthalene-derived coumarin composites, named *f*, *g*, and *h*, and their related compounds contain electron-acceptors and/or electron donors which are conjugated electronically through the compound's backbone. Naphthalene-derived coumarin composites are of particular importance owing to their charge-transfer nature intramolecularly. This resulted in great attention being paid to employing these composites as scaffolds for new drug developmental approaches [13–22].

In this study, a number of novel naphthalene-derived coumarin composites have been synthesised and then tested for their antibacterial and antifungal activity towards a wide range of bacteria and fungi. Begin by synthesising **SA0** from 6-amino-7-chloronaphthalen-2-ol. **SA0** is then used to create **SA1,** which then produces a series of derivatives by reacting the latter with different phenolic derivatives. These products were checked for possible antimicrobial potential towards six aerobic gram-negative bacteria, four anaerobic bacteria, and two fungi species by using the well-known method of broth dilution. In addition, their toxicity to a non-pathogenic bacterial strain (*E. coli*) was investigated to determine the potential toxicity to normal flora. The pre-ADMET online program was also used to obtain in silico pharmacokinetic data for them. The pre-ADMET online programme was also used to obtain *in silico* pharmacokinetic data for them.

Experimental section

Instruments and chemicals

Sigma-Aldrich provided the pathogenic bacterial cultures used in this study, which were experimental in nature. Chemicals, reagents, and solvents were sourced from reputable international suppliers and used without further purifying. The melting points (Mp) of the synthesised composites were determined using the USP-dependent capillary technique on an electrothermal CIA 9300 apparatus. To ensure the purity of the produced agents and the fulfilment of reactions, thin-layer chromatography (TLC) is being utilized, employing typical silica gel aluminium-based plates and also, a combination of chloroform ($CHCl_3$) and propanone (4:1) as an eluting solution. Synthetic composite UV scanning was

conducted by UV-1600PC UV-Vis. Bruker α-ATR-FTIR was used for FTIR scanning. Testing of ^{1}H-and ^{13}C-NMR spectra was done by the Bruker Avance DRX-300 MHz spectrophotometer.

Synthetic protocol

Scheme 1 illustrates the steps for the synthesis of **SA0** and its based composites starting from 6-amino-7-chloro-2-naphthol.

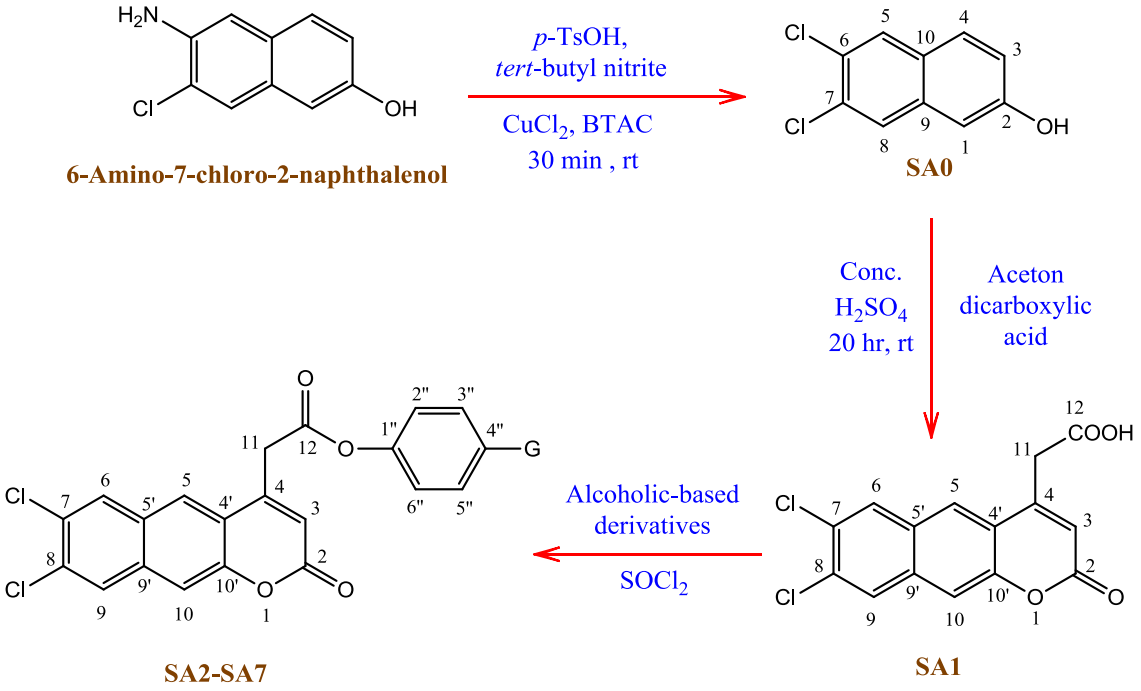

SA2: G= OCH_3; **SA3**: G= CH_3; **SA4**: G= F;
SA5: G= Cl; **SA6**: G= Br; **SA7**: G= I

SCHEME 1 Chemical synthesis of **SA0** and its based composites

Synthesis of SA0

At room temperature (RT), a combination of 6-amino-7-chloro-2-naphthol (5.00 mmol, 0.96 g), triethylbenzylammonium chloride (6.00 mmol, 1.37 g), copper dichloride (0.22 mmol, 0.03 g), 1,1-dimethylethyl nitrite (6.00 mmol, 0.71 mL), and *p*-toluenesulphonic acid (6.00 mmol, 1.03 g) were mixed and milled for 30 minutes using a mortar and pestle. Water and ether were utilized to rinse the mortar separately, using 20 mL of each three times. The prepared crude was recrystallized from aqueous ethyl alcohol after vaporizing the organic phase [23,24].

6,7-Dichloro-2-naphthol (SA0)

White crystals; Yield=52% (0.55 g); Mp=132-134°C; R_f =0.16; λ_{max} (EtOH)=267 nm; IR ν_{max} (cm^{-1}): 3300 (br, phenolic O-H), 3076 (m, aromatic C-H), 2957 (w, alkane C-H), 1561 (s, aromatic C=C), and 915 (s, C-Cl); ^{1}H-NMR (ppm, 300 MHz, DMSO-d_6): δ=8.15 (1H, d, H-4, *J*=9Hz), 7.72 (1H, s, H-5), 7.62 (1H, s, H-8), 7.55 (1H, s, H-1), 7.22 (1H, d, H-3, *J*=9Hz), and 5.56 (1H, s, OH); ^{13}C-NMR (ppm, 75 MHz, DMSO-d_6): δ=158.1 (C, C-2), 135.5 (C, C-9), 132.5 (C, C-7), 131.4 (CH, C-4), 129.8 (C, C-10), 128.7 (C, C-6), 128.3 (CH, C-5), 127.3 (CH, C-8), 120.1 (CH, C-3), and 111.4 (CH, C-1).

Synthesis of SA1

In a conical flask, 25 mL of concentrated sulphuric acid (H_2SO_4) were cooled using an ice bath. When the temperature dropped below 10°C, 2.75 g of **SA0** (13.22 mmol) and 3.5 mL of acetone dicarboxylic acid (15.00 mmol) were mixed, placed in a separatory funnel, and added drop by drop to the chilled H_2SO_4 with stirring. During the addition, the mixture temperature should be kept less than 10°C. After completing the addition, the obtained mixture remained at room temperature (RT) with continuous stirring for 20 hours. Then, it was poured into a beaker containing water and crushed ice and mixed. The formed precipitate was filtered using a filter paper, washed with cold water, and allowed to dry at RT, affording **SA1** composite [25,26].

11-(7,8-Dichloro-2-oxo-2H-benzo[g]chromen-4-yl)acetic acid (SA1)

Pale yellowish powder; Yield= 48% (0.78 g); Mp=154-156 °C; R_f=0.11; λ_{max} (EtOH)=411 nm; IR ν_{max} (cm^{-1}): 3062 (m, *cis* C-H), 3015 (br, carboxylic acid O-H), 2891 (w, alkane C-H), 1734 (s, cyclic ester C=O), 1692 (s, dimeric carboxylic acid C=O), 1590 (s, *cis* C=C), 1548 (m, aromatic C=C), and 941 (s, aromatic C-Cl); ^{1}H-NMR (ppm, 300 MHz, DMSO-d_6): δ=11.09 (1H, s, H-12); 7.92 (1H, s, H-5), 7.72 (1H, s, H-6), 7.60 (1H, s, H-9), 7.12 (1H, s, H-10), 6.35 (1H, s, H-3), and 3.12 (2H, s, H-11); ^{13}C-NMR (ppm, 75 MHz, DMSO-d_6): δ=173.1 (C, C-12), 162.2 (C, C-2), 153.0 (C, C-4), 151.8 (C, C-10'), 132.6 (C, C-9'), 130.1 (C, C-8), 129.0 (CH, C-6), 128.1 (C, C-5'), 127.5 (C, C-4'), 126.0 (C, C-7), 125.5 (CH, C-9), 125.1 (CH, C-5), 115.8 (CH, C-3), 113.4 (CH, C-10), and 30.9 (CH_2, C-11).

Synthesis of SA2-SA7

A two-nick round-bottomed flask containing a mixture of 25 mL of refreshed sulfinyl chloride and 1.60 g of **SA1** (5.00 mmol) was placed in a salt-ice bath. A stopper containing blue litmus test paper was used to confine the side-nick, while a condenser was attached to the centre. Then, the mixture was stirred gently under anhydrous conditions for 30 minutes, followed by stirring for an additional 30 minutes at RT. After that, the obtained mixture was refluxed for 3 hours. A litmus test paper, which was replaced every 30 minutes, was used to detect the reaction's progress. The excess of sulfinyl chloride was distilled out when the colour of the litmus paper remained blue. The **SA1** acyl congener remained in the concave of the flask as a white solid substance [27,28].

Under water-free conditions, a solution of 4.80 mmol of phenolic derivative with 1 mL of pyridine in 50 mL of anhydrous ethoxyethane was poured into the same flask and stirred for 30 minutes at RT. The refluxing of the mixture is continued for some time until the colour of the litmus paper remains blue. After that, 50 mL of water was added to the mixture. The organic layer was then isolated, dried, and vaporized. A 1:2 mixture of propane and methylene dichloride was used for the recrystallization to obtain the **SA1** composite [29,30].

4''-Methoxyphenyl-11-(7,8-dichloro-2-oxo-2H-benzo[g]chromen-4-yl)acetate (SA2)

Off-white powder; Yield= 78% (1.08 g); Mp= 146-148°C; R_f=0.32; λ_{max} (EtOH)=345 nm; IR ν_{max} (cm^{-1}): 3096 (m, *cis* C-H), 2917 (w, methoxy C-H), 2821 (w, alkane C-H), 1731 (s, cyclic ester C=O), 1710 (s, acyclic ester C=O), 1665 (s, *cis* C=C), 1595 (s, aromatic C=C), 1216 and 1144 (s, aryl-alkyl ether C-O-C), and 985 (s, aromatic C-Cl); ^{1}H-NMR (ppm, 300 MHz, DMSO-d_6): δ=7.92 (1H, s, H-5), 7.72 (1H, s, H-6), 7.60 (1H, s, H-9), 7.12 (1H, s, H-10), 7.01 (2H, d, *J*=6Hz, H-3'', 5''), 6.74 (2H, d, *J*=6Hz, H-2'',6''), 6.35 (1H, s, H-3), 4.12 (3H, s, OCH_3 -4''), and 3.12 (2H, s, H-11); ^{13}C-NMR (ppm, 75 MHz, DMSO-d_6): δ=169.5 (C, C-12), 162.2 (C, C-2), 156.4 (C, C-4''),153.0 (C ,C-4),

151.8 (C, C-10'), 144.6 (C, C-1''), 132.6 (C, C-9'), 130.1 (C, C-8), 129.0 (CH, C-6), 128.1 (C, C-5'), 127.5 (C, C-4'), 126.4 (CH, C-9), 125.1 (CH, C-5), 124.0 (C, C-7), 120.1 (CH, C-3'',5''), 115.8 (CH, C-3), 113.4 (CH, C-10), 112.3 (CH, C-2'',6''), 51.1 (CH_3, OCH_3-4''), and 28.3 (CH_2 ,C-11).

4''-Tolyl-11-(7,8-dichloro-2-oxo-2H-benzo[g]chromen-4-yl)acetate (SA3)

Pale yellowish powder; Yield=72% (1.11 g); Mp=138-140°C; R_f =0.30; λ_{max} (EtOH)=398 nm; IR ν_{max} (cm^{-1}): 3090 (m, *cis* C-H), 2877 and 2818 (w, alkane C-H), 1733 (s, cyclic ester C=O), 1713 (s, acyclic ester C=O), 1668 (s, *cis* C=C), 1597 (s, aromatic C=C), and 985 (s, aromatic C-Cl); ^{1}H-NMR (ppm, 300 MHz, DMSO-d_6): δ=7.92 (1H, s, H-5), 7.72 (1H, s, H-6), 7.60 (1H, s, H-9), 7.25 (2H, d, *J*=6Hz, H-3'',5''), 7.12 (1H, s, H-10), 7.02 (2H, d, *J*=6Hz, H-2'',6''), 6.35 (1H ,*s* , H-3), 3.12 (2H, s, H-11), and 2.75 (3H, s, CH_3-4''); ^{13}C-NMR (ppm, 75 MHz, DMSO-d_6): δ=169.5 (C, C-12), 162.2 (C, C-2), 153.0 (C, C-4), 151.8 (C, C-10'), 149.3 (C, C-1''), 134.2 (C, C-4''), 132.6 (C, C-9'), 130.1 (C, C-8), 129.1 (CH, C-6), 128.1 (C, C-5'), 127.5 (C, C-4'), 126.4 (CH, C-9), 125.1 (C, CH-5), 124.0 (C, C-7), 122.0 (CH, C-3'',5''), 119.0 (CH, C-2'',6''), 115.8 (CH, C-3), 113.4 (CH, C-10), 27.5 (CH_2, C-11), and 24.1 (CH_3 ,CH_3-4'').

4''-Fluorophenyl-11-(7,8-dichloro-2-oxo-2H-benzo[g]chromen-4-yl)acetate (SA4)

White powder; Yield=42% (1.13 g); Mp= 144-148°C; R_f=0.21; λ_{max} (EtOH)=316 nm; IR ν_{max} (cm^{-1}): 3070 (m, *cis* C-H), 2820 (w, alkane C-H), 1733 (s, cyclic ester C=O), 1711 (s, acyclic ester C=O), 1666 (s, *cis* C=C), 1597 (s, aromatic C=C), 1077 (s, aromatic C-F), and 986 (s, aromatic C-Cl); ^{1}H-NMR (ppm, 300 MHz, DMSO-d_6): δ=7.92 (1H, s, H-5), 7.72 (1H, s, H-6), 7.60 (1H, s, H-9), 7.26 (2H, d, *J*=6Hz, H-2'',6''), 7.12 (1H, s, H-10), 7.04 (2H, d, *J*=6Hz, H-3'',5''), 6.35 (1H, s, H-3), and 3.12 (2H, s, H-11); ^{13}C-NMR (ppm, 75 MHz, DMSO-d_6): δ=169.5 (C, C-12), 162.2 (C, C-2), 158.7 (C, C-4''), 153.0 (C, C-4), 151.8 (C, C-10'), 147.9 (C, C-1''), 132.6 (C, C-9'), 130.1 (C, C-8), 129.0 (CH, C-6), 128.1 (C, C-5'), 127.5 (C, C-4'), 126.4 (CH, C-9), 126.0 (C, C-5), 125.1 (CH, C-7), 120.7 (CH, C-2'',6''), 115.8 (CH, C-3), 113.4 (CH, C-10), 108.5 (CH,C-3'',5''), and 27.5 (CH_2, C-11).

4''-Chlorophenyl-11-(7,8-dichloro-2-oxo-2H-benzo[g]chromen-4-yl)acetate (SA5):

Off-white powder; Yield= 43% (1.03 g); Mp=133-135°C; R_f=0.24; λ_{max} (EtOH)=374 nm; IR ν_{max} (cm^{-1}): 3068 (m, *cis* C-H), 2820 (w, alkane C-H), 1730 (s, cyclic ester C=O), 1710 (s, acyclic ester C=O), 1667 (s, *cis* C=C), 1595 (s, aromatic C=C), and 985 (s, aromatic C-Cl); ^{1}H-NMR (ppm, 300 MHz, DMSO-d_6): δ=7.92 (1H, s, H-5), 7.72 (1H, s, H-6), 7.60 (1H, s, H-9), 7.53 (2H, d, *J*=6Hz, H-3'',5''), 7.35 (2H, d, *J*=6Hz, H-2'',6''), 7.12 (1H, s, H-10), 6.35 (1H, s, H-3), and 3.12 (2H, s, H-11); ^{13}C-NMR (ppm, 75 MHz, DMSO-d_6): δ=169.5 (C, C-12), 162.2 (C, C-2), 153.0 (C, C-4), 151.8 (C, C-10'), 150.4 (C, C-1''), 132.6 (C, C-9'), 132.0 (C, C-4''), 130.1 (C, C-8), 129.0 (CH, C-6), 128.1(C, C-5'), 127.5(C, C-4'), 126.4 (CH, C-9), 126.0 (C, C-7), 125.1 (CH, C-5), 122.9 (CH, C-3'',5''), 120.5 (CH, C-2'',6''), 115.9 (CH, C-3), 113.4 (CH, C-10), and 33.2 (CH_2, C-11).

4''-Bromophenyl-11-(7,8-dichloro-2-oxo-2H-benzo[g]chromen-4-yl)acetate (SA6)

Pale yellowish powder; Yield=42% (1.1 g); Mp=123-125°C; R_f=0.28; λ_{max} (EtOH)=409 nm; IR ν_{max} (cm^{-1}): 3066 (m, *cis* C-H), 2819 (w, alkane C-H), 1732 (s, cyclic ester C=O), 1709 (s, acyclic ester C=O), 1664 (s, *cis* C=C), 1593 (s, aromatic C=C), 986 (s, aromatic C-Cl), and 900 (s, C-Br); ^{1}H-NMR (ppm, 300 MHz, DMSO-d_6): δ=7.92 (1H, s, H-5), 7.77 (2H, d, *J*=6Hz, H-3'',5''), 7.72 (1H, s, H-6), 7.60 (1H, s, H-9), 7.11 (1H, s, H-10), 6.95 (2H, d, *J*=6Hz, H-2'',6''), 6.35 (1H, s, H-3), and 3.13 (2H, s, H-11); ^{13}C-NMR (ppm, 75 MHz, DMSO-d_6): δ=169.5 (C, C-12), 162.2 (C, C-2), 153.0 (C, C-4), 151.8 (C, C-10'), 151.3 (C, C-1''), 132.6 (C,

C-9'), 130.2 (C, C-8), 129.0 (CH, C-6), 128.1 (C, C-5'), 127.5 (C, C-4'), 126.4 (CH, C-9), 126.0 (C, C-7), 125.1 (CH, C-5), 123.6 (CH, C-3'',5''), 121.3 (CH, C-2'',6''), 118.5 (C, C-4''), 115.8 (CH, C-3), 113.4 (CH, C-10), and 33.2 (CH_2, C-11).

4''-Iodophenyl-11-(7,8-dichloro-2-oxo-2H-benzo[g]chromen-4-yl)acetate (SA7)

Gray-like powder; Yield=43% (1.3 g); Mp=112-114°C; R_f=0.29; λ_{max} (EtOH)=326 nm; IR ν_{max} (cm^{-1}): 3064 (m, *cis* C-H), 2823 (w, alkane C-H), 1733 (s, cyclic ester C=O), 1711 (s, acyclic ester C=O), 1661 (s, *cis* C=C), 1592 (s, aromatic C=C), 986 (s, aromatic C-Cl), and 800 (s, aromatic C-I); ^{1}H-NMR (ppm, 300 MHz, DMSO-d_6): δ= 7.92 (1H, s, H-5), 7.85 (2H, d, *J*=6Hz, H-3'',5''), 7.72 (1H, s, H-6), 7.60 (1H, s, H-9), 7.11 (1H, s, H-10), 6.83 (2H, d, *J*=6Hz, H-2'',6''), 6.35 (1H, s, H-3), and 3.13 (2H, s, H-11); ^{13}C-NMR (ppm, 75 MHz, DMSO-d_6): δ=169.5 (C, C-12), 162.2 (C, C-2), 153.0 (C, C-4), 151.8 (C, C-10'), 151.2 (C, C-1''), 132.6 (C, C-9'), 130.1 (C, C-8), 129.6 (C, CH, C-3'',5''), 129.0 (CH, C-6), 128.1 (C, C-5'), 127.5 (C, C-4'), 126.4 (CH, C-9), 126.0 (C, C-7), 125.1 (CH, C-5), 120.7 (CH, C-2'',6''), 115.8 (CH, C-3), 113.4 (CH, C-10), 93.0 (C, C-4''), and 33.1 (CH_2, C-11).

Theoretical pharmacokinetic factors

By using the web application pre-ADMET (https://preadmet.qsarhub.com/adme/), the pharmacokinetic characteristics of the synthesized naphthalene-derived coumarin composites **SA0**-**SA7** were analysed *in silico*. This analysis involved their absorption, distribution, metabolism, and excretion [31,32].

In-vitro biological potentials

Assessment of the activity towards aerobic Gram negative bacteria

This activity was assessed using the method of broth-dilution. As a growth medium, Mueller-Hinton broth (MHB) was employed. Ciprofloxacin (CPF) was used as a reference and methyl sulfoxide (DMSO) as a negative qualifying agent. 2 mL of the testing composite with a concentration of 100 mg/mL was allowed to dry first, and the remaining was evaluated.

By mixing 7.5 mg of the remnant with 5 mL of methyl sulfoxide, the mother solution was obtained. Then, using autoclaved distilled water as a thinning liquid, a series of 13 two-fold dilutions with a range of labelled concentrations of between 1024 and 0.25 µg/mL were established. 3 mL of MHB, 0.2 mL of inoculant diluted to 0.5 McFarland with autoclaved distilled water, and 1 mL of a predetermined concentration were placed into a labelled test tube as a pre-incubation solution. An examination for the growth of bacteria was done after incubation for 24 hours at 37°C using the naked eyes. The preceding scientific techniques were repeated by the use of diluted amounts based on the values of 4, 1, 0.5, or 0.05, depending on which concentration demonstrated insignificant bacterial multiplication. The Minimum Inhibitory Concentration (MIC), which is measured in micrograms per millilitre, was determined in the last stage as the first microbiological variable [33,34].

The minimum aerobic bactericidal concentration (MABC), which was the second microbiological variable, was also examined. In this case, 3 mL of MHB were incubated with 0.5 mL of the diluted concentration from the second row. Then, the potency factor (PF), which is the third microbiological variable, was determined by dividing the MBC value over the MIC value. It was calculated for each extract towards each utilised bacterium. To optimise the findings, the approach used was tripled [35–37].

Assessment of the activity towards anaerobic bacteria

Although some noticeable changes existed, the approach used to test the activity of the synthesised composites towards anaerobic pathogenic bacteria was similar to the one used to evaluate activity towards aerobic pathogenic bacteria. The microbiological variables are the same except for the abbreviation MABC, which stands for minimum anaerobic bactericidal concentration. The differences were in applying Brucella-agar supplemented with sheep blood (5%) as a growth medium and using Metronidazole (MNZ) as a reference. Furthermore, culture incubation was done in a container that included an anaerobic milieu (10% CO_2, 10% H_2, and 80% N_2), an anaerobe marker, and a metal catalyst (palladium) for 48 hours at 37°C [38].

Assessment of the activity towards pathogenic fungi

The fungicidal influence of the synthesised composites was assessed using an approach which differed slightly from the one used to evaluate their activity towards aerobic bacteria. The microbiological variables are the same except for the abbreviation MFC, which stands for minimum fungicidal concentration. The growth medium of the Sabouraud-dextrose broth was utilised. Nystatin (NYS) was used as a reference agent. The incubation period was 48 hours at 30°C [39].

Results and discussion

Synthetic pathway

The schematic chemical synthesis for **SA0**-**SA7** composites was depicted in Scheme 1. Firstly, **SA0** was synthesised by reacting 6-amino-7-phenolchloro-2-naphthol, triethylbenzylammonium chloride, copper dichloride, 1,1-dimethylethyl nitrite, and *p*-toluenesulphonic acid together by an aromatic nucleophilic substitution reaction. Calcium chloride anhydrous was used for drying the organic face, followed by the sample's recrystallization from aqueous ethyl alcohol. [40].

Concerning **SA1**, which is the precursor of **SA2**–**SA7** composites, the synthesis method involves the condensation of **SA0** composite and acetone dicarboxylic acid with the aid of concentrated H_2SO_4 via a Pechmann type condensation reaction. This reaction is considered the most widely used one for the synthesis of coumarin-related compounds. With the aid of a condensing agent, the starting materials utilised in this reaction are simple and include β-carbonyl group-containing ester and phenol. The nature of the resulted product and its yield depend on the reactant's reactivity and type. The last step, the synthesis of **SA2**–**SA7** composites included converting the carboxylic acid moiety of the **SA1** composite into an acid chloride-derived product by reacting with $SOCl_2$. The reaction of the produced intermediate with phenolic derivatives leads to the formation of the final composites. Each one had a different group substituted at the *para*-position of the benzene ring. These groups are methoxy for **SA2**, methyl for **SA3**, fluoride for **SA4**, chloride for **SA5**, bromide for **SA6**, and iodide for **SA7** [16]. Only a few studies exist in the literature aiding the use of halophenol as a starting material in this type of reaction because the nucleophilicity of this form of phenol is poor due to the deactivation effect of the halogen attached to it. In this work, the yields of the synthesized **SA2**–**SA7** composites were improved by precise monitoring of the reaction conditions [21].

Theoretical pharmacokinetic parameters

As drug discovery and development are very complex and diverse processes, a number of *in silico* evaluations have been created to offer data on the pharmacokinetic characteristics of the compounds under

investigation [26]. The examination of the parameters listed in Table 1 revealed a number of interesting points, including that these novel naphthalene-derived coumarin composites have high HIA percentages ranging from 97.69% to 100.00%, indicating a high theoretical oral bioavailability. They have moderate Caco2 cell permeability with P-glycoprotein (Pggp-1) inhibiting capability. These parameters can indicate good intestinal absorption for these composites. On the other hand, the inhibitory capacity of these naphthalene-derived coumarin composites towards the CYP2C9 enzyme could suggest good anti-inflammatory activity as this enzyme produces eicosatrienoic acid epoxide, which is an inflammatory signalling molecule, from arachidonic acid metabolism, while the inhibition of CYP3A4 by these composites (except **SA1**) can result in a decrease in the metabolism of some toxins, including the parent drug, which leads to its accumulation and an increased risk of toxicity. Moreover, this action can affect the metabolism of other drugs taken simultaneously with these composites, leading to drug-drug interaction [30]. Additionally, the produced naphthalene-derived coumarin composites have a very high plasma protein binding capacity, which can result in a decrease in the volume of distribution and a reduction in the half-life of these composites [37]. Finally, the poor penetration across the blood-brain barrier (except for **SA0**) might mean that these composites will have low toxicity as a result of a lack of neurological side effects. This limited number of adverse effects is critical in determining CNS toxicity [37].

TABLE 1 Theoretical pharmacokinetic parameters for the **SA0**-**SA7** composites

Symbol	Caco2 -P	PPB	CYP2C9	CYP2D 6	CYP3A4	Pggp-1	HIA	BBB-P	Rule Of five
SA0	38.41	98.99	Inhibitor	Non	Inhibitor	Inhibitor	100.0 0	6.61	Yes; 0 violation
SA1	15.19	95.68	Inhibitor	Non	Non	Inhibitor	97.75	0.06	Yes; 0 violation
SA2	36.42	96.18	Inhibitor	Non	Inhibitor	Inhibitor	97.69	0.11	Yes; 1 violation: MLOGP>4.15
SA3	36.40	97.51	Inhibitor	Non	Inhibitor	Inhibitor	97.87	0.33	Yes; 1 violation: MLOGP>4.15
SA4	36.26	100.00	Inhibitor	Non	Inhibitor	Inhibitor	97.82	0.14	Yes; 1 violation: MLOGP>4.15
SA5	38.99	100.00	Inhibitor	Non	Inhibitor	Inhibitor	98.04	0.21	Yes; 1 violation: MLOGP>4.15
SA6	36.91	100.00	Inhibitor	Non	Inhibitor	Inhibitor	98.15	0.23	Yes; 1 violation: MLOGP>4.15
SA7	35.56	100.0	Inhibitor	Non	Inhibitor	Inhibitor	98.31	0.23	No; 2 violations: MW>500, MLOGP>4.15

Antimicrobial activity

In this research, the activity of the synthesized naphthalene-derived coumarin composites as antibacterial and antifungal applicants was assessed using the famous method of broth-dilution. Three antimicrobial variables were measured, namely: MIC, MABC (or MFC for fungi), and PF. The values for aerobic gram-negative bacteria, anaerobic bacteria, and fungi are listed in Tables 2, 3, and 4, respectively.

Aerobic gram negative bacteria

The pathogenic aerobic gram-negative bacterial strains used in this study were *Klebsiella pneumonia* (700603-ATCC, *K-pneumonia*), *Pseudomonas aeruginosa* (27853-ATCC, *P-aeruginosa*), *Escherichia coli* (25922-ATCC, *E-coli*), *Haemophilus influenzae* (49247-ATCC, *H-influenzae*), *Shigella dysenteriae* (13313-ATCC, *S-dysenteriae*), *Salmonella typhi* (6539-ATCC, *S-typhi*), as well as the non-pathological *Escherichia coli* strain

(BAA-1427, *E-coli*) to determine the safety of the synthesized composites.

The first observation was made concerning the pathological bacterial strains that all of the synthesized naphthalene-derived coumarin composites have a weaker bactericidal influence towards the tested pathogens compared to the reference, CPF. The second is that these composites have bactericidal influence in the following order: **SA4** > **SA5** > **SA0** > **SA2** > **SA3** > **SA6** > **SA7** > **SA1**. **SA4** has the strongest activity among these composites. This may be attributed to the fluoride moiety which is considered one of the most powerful electron-withdrawing substitutions leading to the formation of a more active compound. The diagrams of their MIC, MBC, and AE are displayed in Figures 1, 2, and 3, respectively.

Another two observations were obtained from testing the synthesised naphthalene-derived coumarin composites' effects on normal flora to determine their safety profile. The first is that all of them have less toxicity towards the normal floral *E. coli* strain compared to CPF. The second is that the order of toxicity of these composites, starting from the least toxic one, is as follows: **SA5** < **SA4** < **SA1** < **SA2** < **SA3** < **SA6** < **SA7** < **SA0**. The MIC, MABC, and PF diagrams are illustrated in Figures 4, 5, and 6, respectively.

TABLE 2 Bactericidal influence of **SA0-SA7** composites towards gram-negative aerobic bacteria

Aerobic gram-negative bacteria	Microbiological variable	Symbols of the standard and tested synthetic composites								
		CPF	SA0	SA1	SA2	SA3	SA4	SA5	SA6	SA7
K-pneumonia ATCC 700603	MIC	0.40	3.95	9.15	4.80	6.00	1.95	2.25	5.85	7.35
	MABC	0.45	4.75	9.95	5.35	6.60	2.10	2.60	6.25	7.60
	PF	1.13	1.20	1.09	1.11	1.10	1.08	1.16	1.07	1.03
P-aeruginosa ATCC 27853	MIC	0.75	3.60	7.30	4.05	4.00	2.05	2.55	5.15	5.90
	MABC	0.85	4.15	8.05	4.70	4.80	2.30	2.70	5.60	6.30
	PF	1.13	1.15	1.10	1.16	1.20	1.12	1.06	1.09	1.07
E-coli ATCC 25922	MIC	0.85	4.15	10.60	5.25	6.05	2.65	3.05	6.70	7.80
	MABC	0.95	4.90	10.95	5.90	6.55	2.90	3.50	6.95	8.05
	PF	1.12	1.18	1.03	1.12	1.08	1.09	1.15	1.04	1.03
H-influenza ATCC 49247	MIC	0.60	3.60	9.45	4.95	5.25	2.15	2.90	6.15	7.05
	MABC	0.65	4.05	10.05	5.55	5.90	2.30	3.15	6.40	7.35
	PF	1.08	1.13	1.06	1.12	1.12	1.07	1.09	1.04	1.04
S-dysenteriae ATCC 13313	MIC	0.55	4.20	10.80	5.70	7.30	2.00	3.05	7.25	9.05
	MABC	0.80	4.90	11.15	6.10	7.95	2.10	3.40	7.55	9.75
	PF	1.45	1.17	1.03	1.07	1.09	1.05	1.11	1.04	1.08
S-typhi ATCC 6539	MIC	0.80	4.20	10.55	5.85	7.10	2.50	3.70	8.00	9.25
	MABC	1.00	4.95	11.00	6.30	7.45	2.65	3.95	8.40	9.80
	PF	1.25	1.18	1.04	1.08	1.05	1.06	1.07	1.05	1.06
E-coli BAA-1427	MIC	0.90	3.80	14.00	8.00	7.00	14.00	16.00	4.50	4.50
	MABC	0.95	5.00	18.00	12.00	8.00	60.00	52.00	7.00	7.00
	PF	1.06	1.32	1.29	1.50	1.14	4.29	3.25	1.56	1.56

All findings are demonstrated in terms of μg/mL

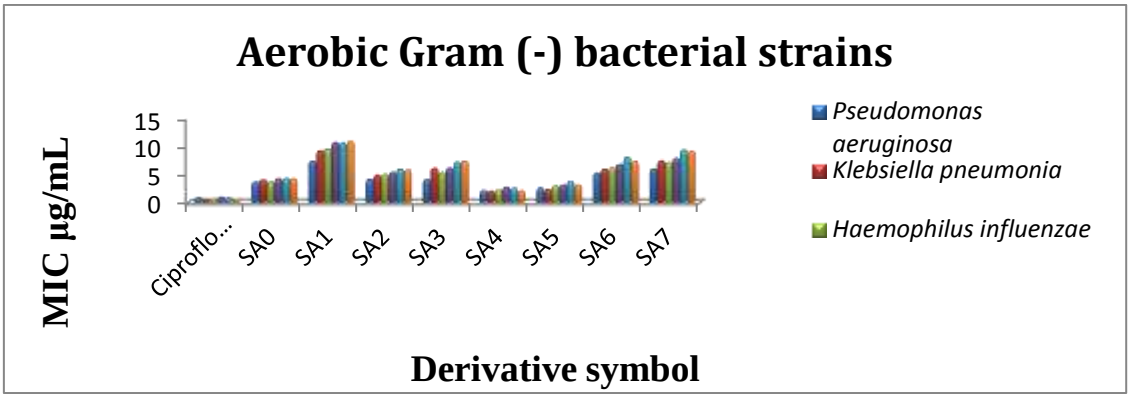

FIGURE 1 Diagram showed the MIC values of **SA0-SA7** composites towards gram (-) aerobic bacteria

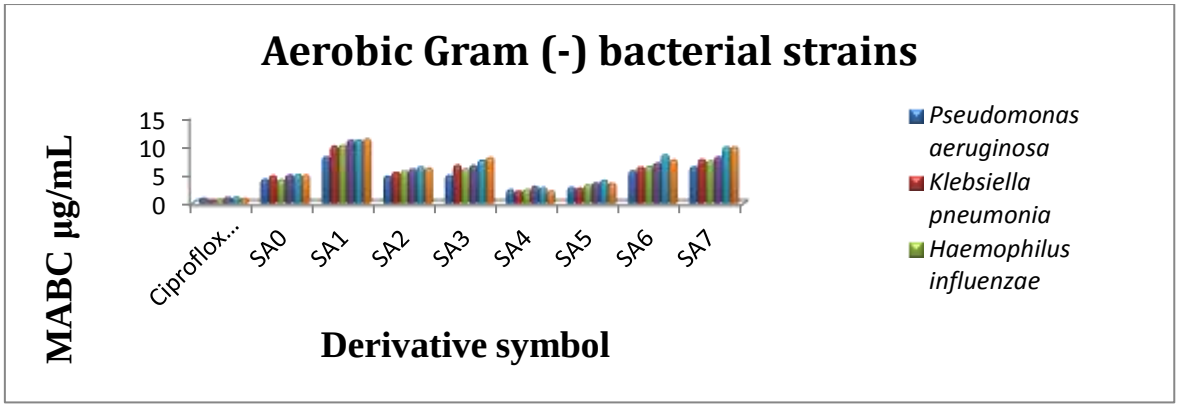

FIGURE 2 Diagram indicates the MBC values of **SA0-SA7** composites towards gram (-) aerobic bacteria

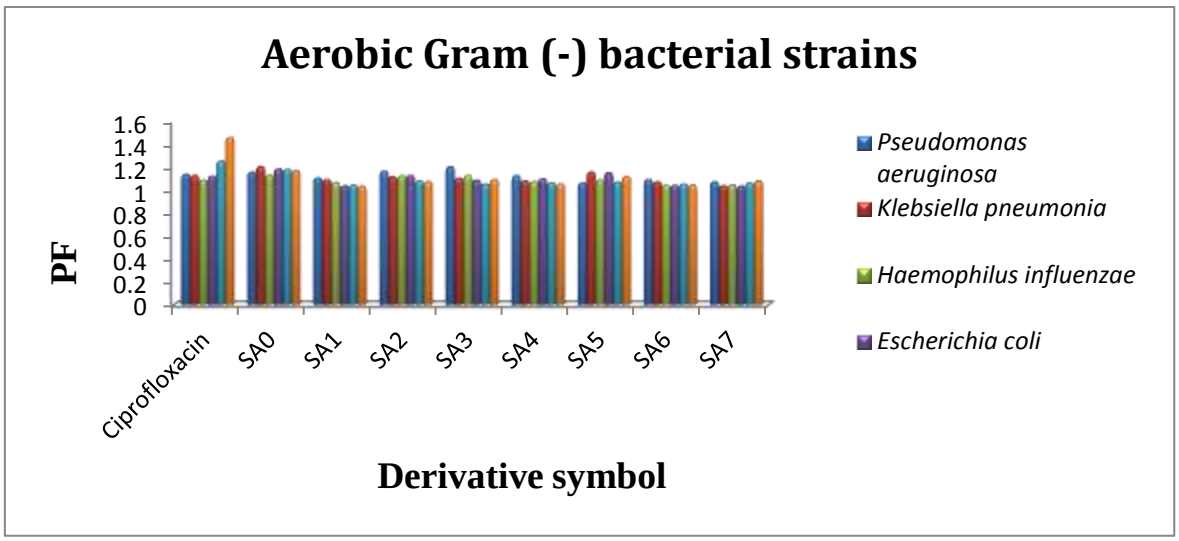

FIGURE 3 Diagram demonstrates the AE values of **SA0-SA7** composites towards gram (-) aerobic bacteria

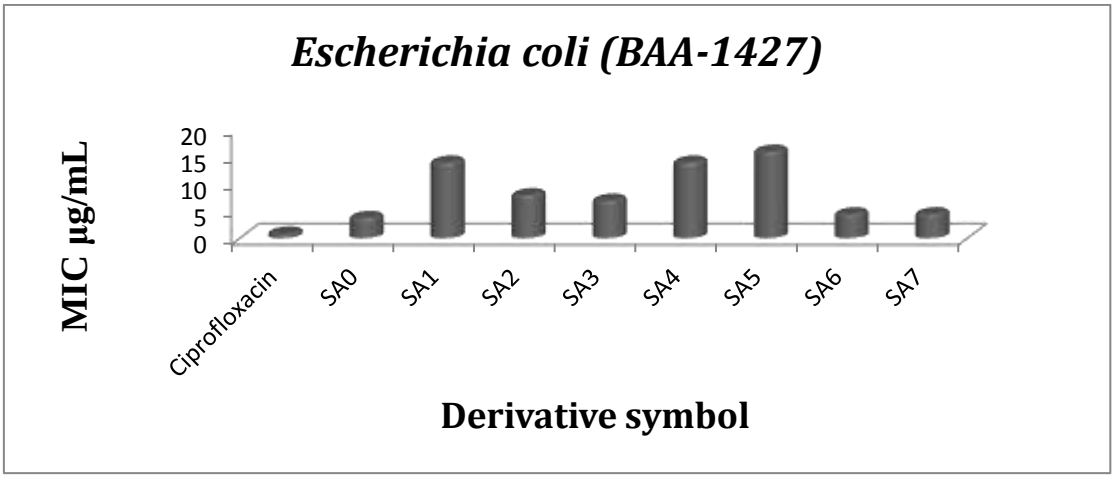

FIGURE 4 Diagram illustrates the MIC values of **SA0-SA7** towards normal flora

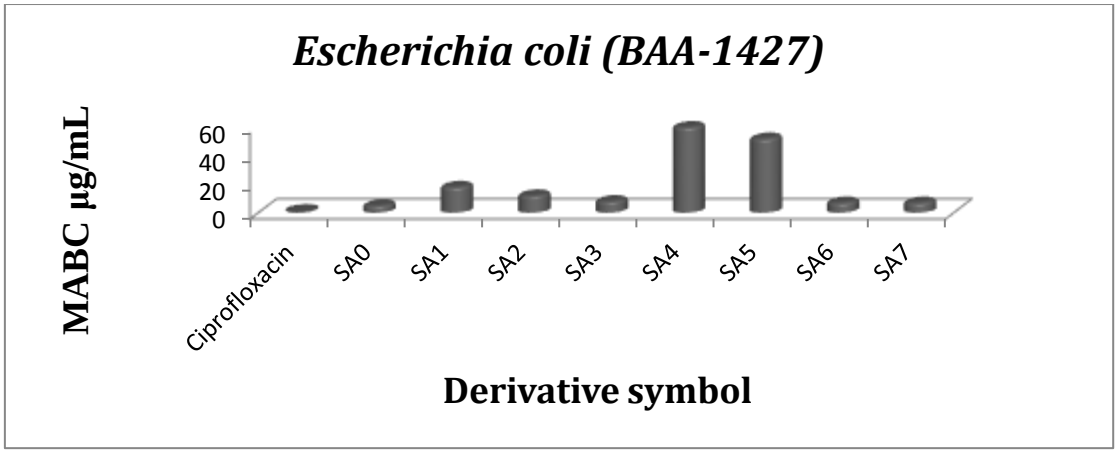

FIGURE 5 Diagram reveals the MABC values of **SA0-SA7** composites towards normal flora

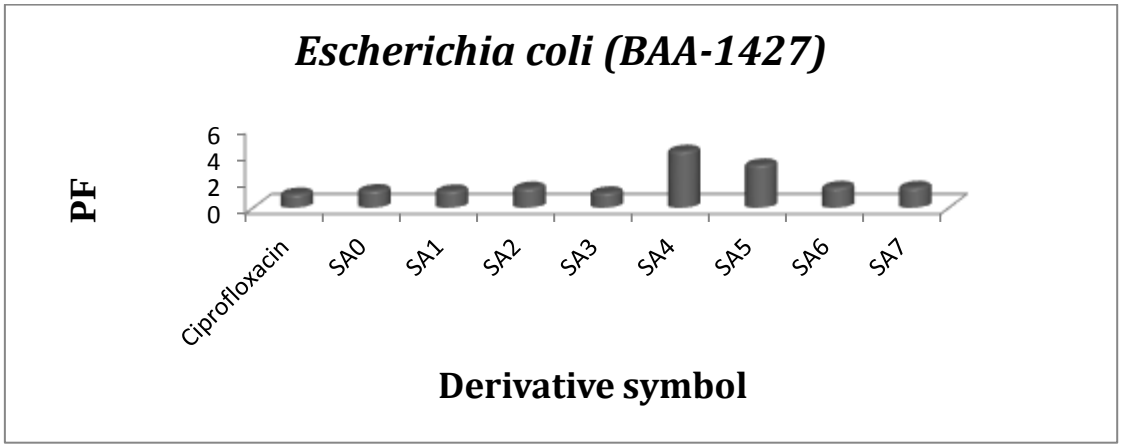

FIGURE 6 Diagram shows the PF values of **SA0-SA7** composites towards normal flora.

Anaerobic bacteria

Four anaerobic pathogenic bacterial strains were utilized in this work, namely *Clostridium perfringens* (13124-ATCC, *C-perfringens*), *Bacteroides fragilis* (25285-ATCC, *B-fragilis*), *Prevotella melaninogenica* (25845-ATCC, *P-melaninogenica*), and *Fusobacterium necrophorum* (25286-ATCC, *F-necrophorum*).

All of the tested naphthalene-derived coumarin composites have much less activity compared with MNZ, the standard drug. The order of their bactericidal influence is: **SA4** > **SA5** > **SA2** > **SA3** > **SA0** > **SA6** > **SA7** > **SA1**. Diagrams for the three microbiological variables are shown in Figures 7, 8, and 9, respectively.

TABLE 3 Bactericidal influence of **SA0-SA7** composites towards anaerobic bacteria

Anaerobic bacteria	Microbiological variable	Symbols of the standard and tested synthetic composites								
		MNZ	SA0	SA1	SA2	SA3	SA4	SA5	SA6	SA7
C-perfringens ATCC 13124	MIC	0.75	52.00	48.00	48.00	56.00	36.00	40.00	48.00	52.00
	MABC	0.95	54.00	50.00	49.00	58.00	38.00	43.00	53.00	55.00
	PF	1.27	1.04	1.04	1.02	1.04	1.06	1.08	1.10	1.06
B-fragilis ATCC 25285	MIC	3.00	40.00	52.00	28.00	32.00	20.00	26.00	44.00	40.00
	MABC	3.50	42.00	55.00	30.00	34.00	21.00	29.00	47.00	42.00
	PF	1.17	1.05	1.06	1.07	1.06	1.05	1.12	1.07	1.05
P-melaninogenica ATCC 25845	MIC	0.75	44.00	64.00	36.00	40.00	30.00	32.00	52.00	60.00
	MABC	0.90	46.00	68.00	39.00	43.00	34.00	38.00	55.00	66.00
	PF	1.20	1.05	1.06	1.08	1.08	1.13	1.19	1.06	1.10
F-necrophorum ATCC 25286	MIC	1.75	56.00	64.00	44.00	56.00	40.00	36.00	60.00	64.00
	MABC	1.80	57.00	68.00	47.00	59.00	43.00	40.00	65.00	69.00
	PF	1.03	1.02	1.06	1.07	1.05	1.08	1.11	1.08	1.08

All findings are demonstrated in terms of µg/mL

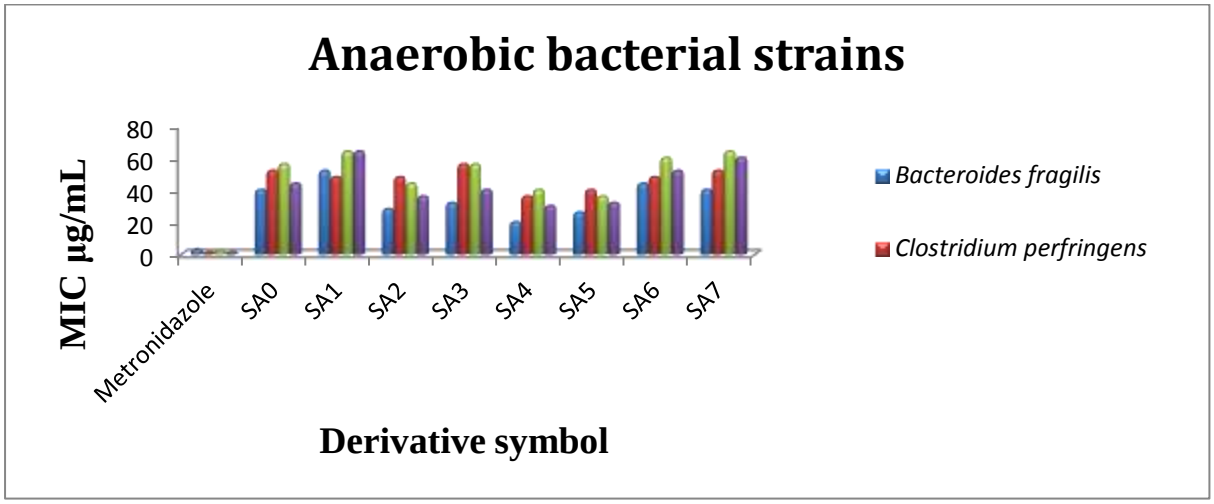

FIGURE 7 Diagram indicates the MIC values of **SA0-SA7** composites towards anaerobic bacteria.

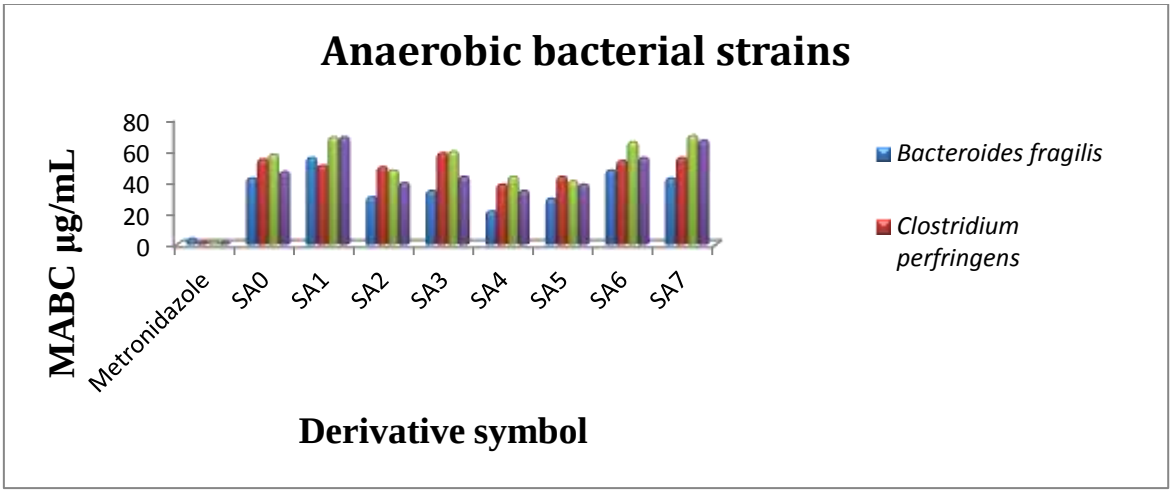

FIGURE 8 Diagram shows the MABC values of **SA0-SA7** composites towards anaerobic bacteria.

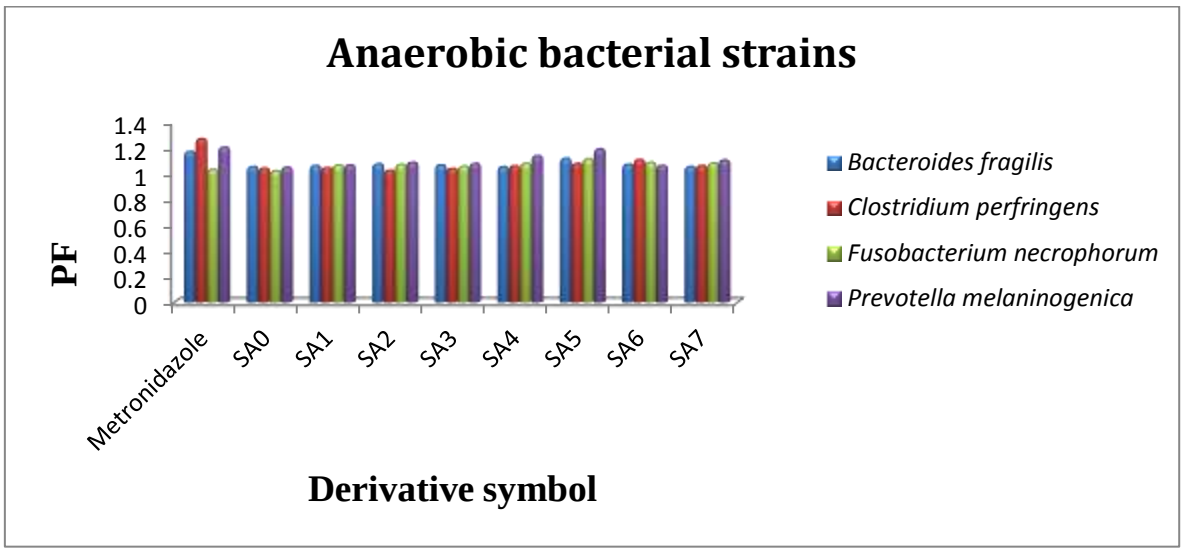

FIGURE 9 Diagram displays the PF values of **SA0-SA7** composites towards anaerobic bacteria.

Pathogenic fungi

The fungicidal influence of these novel naphthalene-derived coumarin composites was tested towards two pathological fungal strains, *Aspergillus niger* (16888-ATCC, *A-niger*) and *Candida albicans* (10231-ATCC, *C-albicans*).

A number of imperative observations are made. The most important one is that most of the synthesised naphthalene-derived coumarin composites (**SA0-SA5**) have very powerful fungicidal influence compared to NYS, as a standard. On the other hand, **SA6** and **SA7** have very weak activity towards the tested fungal strains. This may be attributed to the bromide and iodide moieties in these two composites, which have lower electron withdrawing capacity compared to other substituents, making the compound less active. The sequence of the fungicidal influences of these compounds is as follows: **SA5** > **SA4** > **SA1** > **SA3** > **SA2** > **SA0** >> **SA7** > **SA6**. Diagrams for MIC, MFC, and PF are displayed in Figures 10, 11, and 12, respectively.

TABLE 4 fungicidal influence of **SA0-SA7** composites towards pathogenic fungi

Pathogenic fungi	Microbiological variable	Symbols of the standard and tested synthetic composites								
		NYS	SA0	SA1	SA2	SA3	SA4	SA5	SA6	SA7
A-niger ATCC 16888	MIC	8.00	3.00	2.20	3.50	2.20	2.05	1.85	28.00	24.00
	MFC	12.00	3.25	2.35	3.75	2.45	2.30	1.90	31.00	27.00
	PF	1.50	1.08	1.07	1.07	1.11	1.12	1.03	1.11	1.13
C-albicans ATCC 10231	MIC	4.00	1.95	1.80	2.80	2.25	1.65	1.50	22.00	12.00
	MFC	6.00	2.10	1.85	2.95	2.60	1.75	1.55	24.00	14.00
	PF	1.50	1.08	1.03	1.05	1.16	1.06	1.03	1.09	1.17

All findings are demonstrated in terms of μg/mL

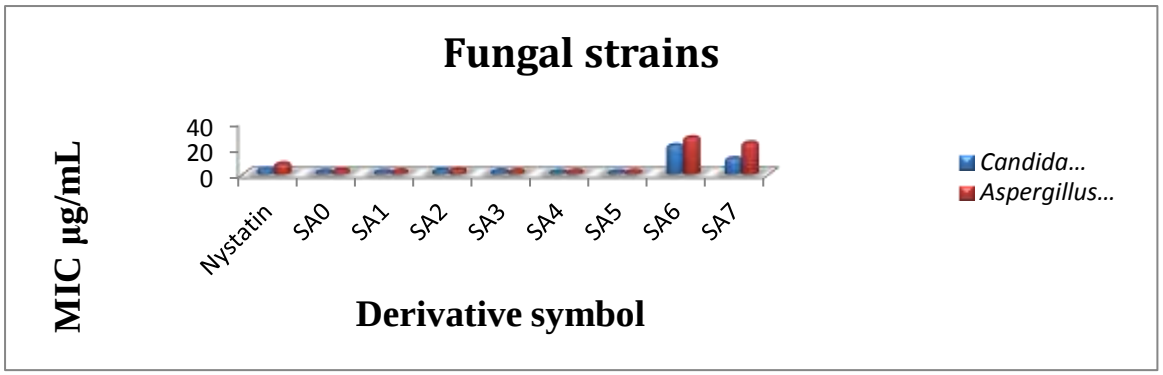

FIGURE 10 Diagram demonstrates the MIC values of **SA0-SA7** composites towards pathogenic fungi

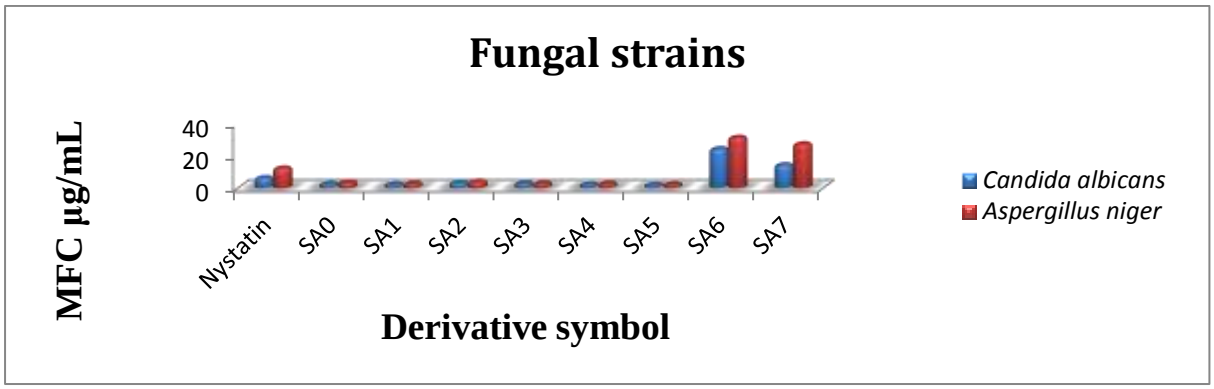

FIGURE 11 Diagram shows the MFC values of **SA0-SA7** composites towards pathogenic fungi

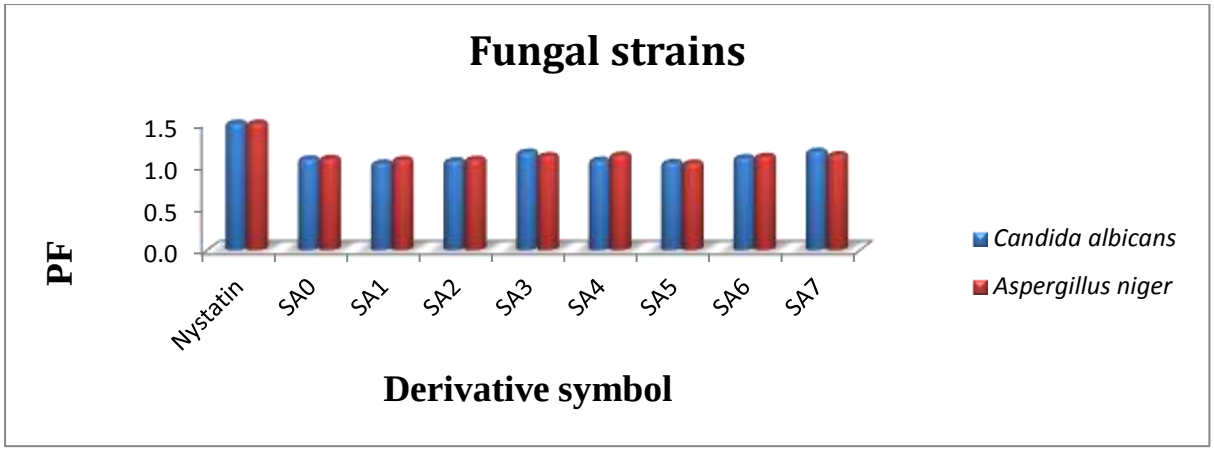

FIGURE 12 Diagram illustrates the PF values of **SA0-SA7** composites towards pathogenic fungi

Conclusion

This work demonstrated the synthesis of eight novel naphthalene-derived coumarin composites from 6-amino-7-phenolchloro-2-naphthol as a starting material. From the pharmacokinetic parameters gathered from the web application pre-ADMET, these composites are shown to have good oral bioavailability, which makes them promising orally administered drugs in the future. The antibacterial and antifungal evaluation of the synthesised naphthalene-derived coumarin composites revealed a number of important observations. Firstly, all of the synthesised derivatives have weak bactericidal influences on gram-negative aerobic bacteria as well as anaerobic bacteria. Secondly, their toxicity profiles towards normal flora are low, which enhances their safety. Thirdly, these composites, except **SA6** and **SA7**, have very strong fungicidal influences. From this finding, along with their good oral absorption profiles, low penetration across the blood-brain barrier, and low toxicity towards normal flora, these new composites could provide a valuable platform for the scanning of new fungicidal drugs.

Acknowledgements

The researchers would like to show appreciation to the Mosul University/Pharmacy College for furnishing this work with various facilities. They would also like to thank Dr. Rahma Mowafaq Jebir, Dr. Sara Firas Jasim, and Dr. Reem Nadher Ismael for their support that help to improve the quality of this work.

Orcid:
Sarah Ahmed Waheed:
https://www.orcid.org/0000-0001-6008-2181
Yasser Fakri Mustafa:
https://www.orcid.org/0000-0002-0926-7428

References

[1] F. Prestinaci, P. Pezzotti, A. Pantosti, *Pathog. Glob. Health.*, **2015**, *109*, 309–318. [Crossref], [Google Scholar], [Publisher]
[2] M.K. Bashir, Y.F. Mustafa, M.K. Oglah, *Syst. Rev. Pharm.*, **2020**, *11*, 175–187. [Google Scholar], [Publisher]
[3] Y.F. Mustafa, R.R. Khalil, E.T. Mohammed, *Egypt. J. Chem.*, **2021**, *64*, 3711–3716. [Crossref], [Google Scholar], [Publisher]
[4] R.R. Khalil, E.T. Mohammed, Y.F. Mustafa, *Clin. Schizophr. Relat. Psychoses*, **2021**, *15*, 1–9. [Google Scholar], [Publisher]
[5] R.R. Khalil, Y.F. Mustafa, *Syst. Rev. Pharm.*, **2020**, *11*, 57–63. [Google Scholar], [Publisher]
[6] H. Lv, P. Tu, Y. Jiang, *Mini-Reviews Med. Chem.*, **2014**, *14*, 603–622. [Crossref], [Google Scholar], [Publisher]
[7] M.K. Oglah, M.K. Bashir, Y.F. Mustafa, E.T. Mohammed, R. Riyadh, *Syst. Rev. Pharm.*, **2020**, *11*, 717–725. [Google Scholar], [Publisher]

[8] Y.F. Mustafa, *J. Med. Chem. Sci.,* **2021**, *4*, 612–625. [Crossref], [Google Scholar], [Publisher]
[9] Y.F. Mustafa, M.K. Oglah, M.K. Bashir, *Syst. Rev. Pharm.,* **2020**, *11*, 482–489. [Google Scholar], [Publisher]
[10] Y.F. Mustafa, N.T. Abdulaziz, *NeuroQuantology,* **2021**, *19*, 175–186. [Google Scholar], [Publisher]
[11] Y.F. Mustafa, *J. Glob. Pharma Technol.,* **2019**, *11*, 1–10. [Google Scholar], [Publisher]
[12] Y.F. Mustafa, M.A. Najem, Z.S. Tawffiq, *J. Appl. Pharm. Sci.,* **2018**, *8*, 49–56. [Crossref], [Google Scholar], [Publisher]
[13] Y.F. Mustafa, R.R. Khalil, E.T. Mohammed, M.K. Bashir, M.K. Oglah, *Arch. Razi Inst.,* **2021**, *76*, 1297–1305. [Crossref], [Google Scholar], [Publisher]
[14] Y.F. Mustafa, N.T. Abdulaziz, *Syst. Rev. Pharm.,* **2020**, *11*, 438–452. [Google Scholar], [Publisher]
[15] H. Aldewachi, Y.F. Mustafa, R. Najm, F. Ammar, *Syst. Rev. Pharm.,* **2020**, *11*, 289–296. [Google Scholar], [Publisher]
[16] Y.F. Mustafa, M.K. Bashir, M.K. Oglah, *Syst. Rev. Pharm.,* **2020**, *11*, 598–612. [Google Scholar], [Publisher]
[17] Y.F. Mustafa, N.A. Mohammed, *Biochem. Cell. Arch.,* **2021**, *21*, 1991–1999. [Google Scholar], [Publisher]
[18] Y.F. Mustafa, E.T. Mohammed, R.R. Khalil, *Egypt. J. Chem.,* **2021**, *64*, 4461–4468. [Crossref], [Google Scholar], [Publisher]
[19] Y.F. Mustafa, M.K. Bashir, M.K. Oglah, R.R. Khalil, E.T. Mohammed, *NeuroQuantology,* **2021**, *19*, 129–138. [Google Scholar], [Publisher]
[20] Y.F. Mustafa, E.T. Mohammed, R.R. Khalil, *Syst. Rev. Pharm.,* **2020**, *11*, 570–576. [Google Scholar], [Publisher]
[21] Y.F. Mustafa, S.M. Kasim, B.M. Al-Dabbagh, W. Al-Shakarchi, *Appl. Nanosci.,* **2021**. [Crossref], [Google Scholar], [Publisher]
[22] M.K. Oglah, Y.F. Mustafa, *J. Glob. Pharma Technol.,* **2020**, *12*, 854–862. [Google Scholar], [Publisher]
[23] Y.F. Mustafa, *NeuroQuantology*, **2021**, *19*, 99–112. [Google Scholar], [Publisher]
[24] M.K. Oglah, Y.F. Mustafa, *Med. Chem. Res.*, **2020**, *29*, 479–486. [Crossref], [Google Scholar], [Publisher]
[25] M.K. Oglah, Y.F. Mustafa, M.K. Bashir, M.H. Jasim, *Syst. Rev. Pharm.*, **2020**, *11*, 472–481. [Google Scholar], [Publisher]
[26] Y.F. Mustafa, *Appl. Nanosci.*, **2021**. [Crossref], [Google Scholar], [Publisher]
[27] M.K. Bashir, Y.F. Mustafa, M.K. Oglah, *Period. Tche Quim.*, **2020**, *17*, 871–883. [Google Scholar], [Publisher]
[28] I. Raya, T. Chen, S.H. Pranoto, A. Surendar, A.S. Utyuzh, S. Al-janabi, A.F. Alkaim, N.T. Danh, Y.F. Mustafa, *Mater. Res.*, **2021**, *24*, e20210245. [Crossref], [Google Scholar], [Publisher]
[29] S. Das, D. Ekka, M. Roy, *Chemical Methodologies.*, **2020**, *4*, 55-67. [Crossref], [Google Scholar] [Publisher]
[30] A.M. Nejres, Y.F. Mustafa, H.S. Aldewachi, *Int. J. Pavement Eng.*, **2022**, *23*, 39–45. [Crossref], [Google Scholar], [Publisher]
[31] E.T. Mohammed, Y.F. Mustafa, *Syst. Rev. Pharm.*, **2020**, *11*, 64–70. [Google Scholar], [Publisher]
[32] E. Nagy, L. Boyanova, U.S. Justesen, *Clin. Microbiol. Infect.,* **2018**, *24*, 1139–1148. [Crossref], [Google Scholar], [Publisher]
[33] Y.F. Mustafa, R.R. Khalil, E.T. Mohammed, *Syst. Rev. Pharm.,* **2020**, *11*, 382–387. [Google Scholar], [Publisher]
[34] A.M. Nejres, , H.K. Ali, , S.P. Behnam, , Y.F. Mustafa, *Syst. Rev. Pharm.,* **2020**, *11*, 726–732. [Google Scholar], [Publisher]
[35] Y.F. Mustafa, , M.K. Oglah, , M.K. Bashir, , E.T. Mohammed, , R.R. Khalil, *Clin. Schizophr. Relat Psychoses,* **2021**, *15*, 1–6. [Google Scholar], [Publisher]
[36] S.O. Hagan, D.B. Kell, *Peer J.*, **2015**, e1405. [Crossref], [Google Scholar], [Publisher]
[37] S.K.D. Kim, J.B.Y. Kim, D.K.H. Lim, C.L. Sang, S. Whang, C.C.J. Bae, Y.J. Lee, C.-G. Jang, S.-Y. Lee, *Arch. Pharm. Res.,* **2017**, *40*, 382–

390. [Crossref], [Google Scholar], [Publisher]
[38] A.B. Roomi, G. Widjaja, D. Savitri, A.T. Jalil, Y.F. Mustafa, L. Thangavelu, G. Kazhibayeva, W. Suksatan, S. Chupradit, S. Aravindhan, *J. Nanostructures,* **2021**, *11*, 514-523. [Crossref], [Google Scholar], [Publisher]
[39] G.K. Dresser, J.D. Spence, D.G. Bailey, *Clin. Pharmacokinet.,* **2000**, *38*, 41–57. [Crossref], [Google Scholar], [Publisher]
[40] L.L. Liu, D. Du, W. Zheng, Y. Zhang, *Neurotoxicology,* **2022**, *88*, 44-56. [Crossref], [Google Scholar], [Publisher]

How to cite this article: Sarah Ahmed Waheed*, Yasser Fakri Mustafa· Novel naphthalene-derived coumarin composites: synthesis, antibacterial, and antifungal activity assessments. *Eurasian Chemical Communications*, 2022, 4(8), 709-724. **Link:** http://www.echemcom.com/article_147424.html